

**Military Technical College  
Kobry El-Kobbah,  
Cairo, Egypt**



**7<sup>th</sup> International Conference  
on Electrical Engineering  
ICEENG 2010**

## **Speckle noise reduction in SAR images using a new morphological filter**

*By*

Ahmed Saleh \*

Ezz Abdelkawy \*

Tarek Mahmoud \*

### **Abstract:**

Speckle noise is one of the most critical disturbances that alter the quality of Synthetic Aperture Radar (SAR) coherent images. Before using SAR images in automatic target detection and recognition, the first step is to reduce the effect of speckle noise. Several adaptive and non-adaptive filters are widely used for despeckling in SAR images. In this paper, a novel mathematical morphological filter is proposed to reduce the speckle noise in SAR images. The new filter performance is compared with a number of despeckling filters with different parameters. For performance measurements, four parameters were evaluated to test the filter ability to attenuate the speckle noise and keep target information. From experimental results, the new proposed morphological filter gives promising results for significantly suppressing speckle noise and preserving the potential targets.

### **Keywords:**

Despeckling filter, Morphological filter and Synthetic Aperture Radar (SAR)

---

\* Egyptian Armed Forces

## **1. Introduction:**

Synthetic Aperture Radar (SAR) is essentially a complicated device whose purpose is simply to measure the local interaction between the Earth's surface and an incident wave. Thus, very high quality SAR images of this interaction can be produced by modern systems. The coherent nature of radar illumination causes the speckle effect, which gives the SAR image its noisy appearance. Thus the produced SAR image is uncomfortable for an untrained eye. For example, consider a regular surface seen by a radar, each image pixel for this surface contains a large number of elementary scatterers, which add their contributions to the field radiated by the pixel in a coherent way. The total pixel response in amplitude and in phase is the result of vector addition of these contributions in the complex plane and is given in Eq.(1)

$$Ae^j = \sum_{k=1}^N A_k e^{j \theta_k} \quad (1)$$

Where  $A \dots$  is the scatters amplitude response.

$\dots$  is the scatters phase response.

$N \dots$  is the total number of scatters in one pixel.

An immediate conclusion from Eq. (1) is that the observed signal will be affected by interference effects as a consequence of the phase differences between scatterers. In fact, speckle can be understood as an interference phenomenon in which the principal source of the noiselike quality of the observed data is the distribution of the phase terms  $\theta_k$ . The sum of Eq. (1) then looks like a random walk in the complex plane, where each step of length  $A_k$  is in a completely random direction [1, 2].

Finally we can say that speckle noise is a granular noise that inherently exists in and degrades the quality of the active radar and SAR images. Speckle noise in conventional radar results from random fluctuations in the return signal from an object that is no bigger than a single image processing element. It increases the mean grey level of a local area. Speckle noise in SAR is generally more serious, causing difficulties for image interpretation. It is caused by coherent processing of backscattered signals from multiple distributed targets.

The remainder of the paper is structured as follows: section 2 presents the speckle noise reduction techniques. Morphology usage in speckle reduction is introduced in section 3. The proposed morphological filter for speckle reduction is described in section 4. Results are presented both as images and image quality metrics are discussed in section 5. Finally, section 6 gives some concluding remarks.

## **2. Speckle Noise Reduction Techniques**

Several different methods are used to eliminate speckle noise, based upon different mathematical models of the phenomenon. One method, for example, employs multiple-look processing, averaging out the speckle noise by taking several "looks" at a target in a single radar sweep, the average is the incoherent average of the looks [1].

A second method involves using adaptive and non-adaptive filters on the image processing (where adaptive filters adapt their weightings across the image to the speckle level, and non-adaptive filters apply the same weightings uniformly across the entire image). Such filtering also eliminates actual image information as well, in particular high-frequency information, and the applicability of filtering and the choice of filter type involve tradeoffs. Adaptive speckle filtering is better at preserving edges and details in high-texture areas (such as forests or urban areas). Non-adaptive filtering is simpler to implement, and requires less computational power [3, 4]. In this paper, we are going to focus on the non-adaptive filters in despeckling SAR images.

### **2.1 Non-Adaptive speckle filtering**

Mean filter (average filter) is a linear filter where the centered pixel's value in its mask depends on the average value of the grey levels neighborhood defined by the filter mask [5].

Median filter is a nonlinear filter where the centered pixel's value in its mask depends on the median value of the grey levels neighborhood defined by the filter mask [5]. The latter is better at preserving edges whilst eliminating noise spikes than the mean filter.

Value-and-criterion filter is a non-adaptive filter which having a "value" function (V) and a "criterion" function (C), each operating separately on the original image, and a "selection" operator (S) acting on the output of (C). The selection operator (S) chooses a location from the output of (C), and the output of (V) at that point is the output of the overall filter. The value-and-criterion structure allows the use of different linear and nonlinear elements in a single filter [6]. Minimum Coefficient of Variant (MCV) filter is an example of the value-and-criterion filter. The MCV filter, therefore, has V= sample mean, C= sample coefficient of variation, and S= minimum of the sample coefficient of variation. At every point in an image, this filter effectively selects the  $n \times n$  subwindow with an overall window  $(2n-1 \times 2n-1)$  that has the smallest measured coefficient of variation, and outputs the mean of that subwindow [7].

### **3. Morphology Usage In Speckle Noise Reduction**

#### **3.1 Introduction to mathematical morphology in grey scale images**

Morphological filters are nonlinear signal transformations that locally modify geometric features of signals. They stem from the basic operations of a set-theoretical method for image analysis, called mathematical morphology, which was introduced by Matheron [8], Serra [9] and Maragos and Schafer [10].

For any morphological filter, we have to define the structuring element to be used and the operation to be performed. For the structuring element, it is used as a “probe” to examine a given image for specific properties. Structuring elements in the grey scale morphology belong to one of two categories: flat and non flat. For the morphological operations, there are only two non linear basic operations: Erosion (minimum) and dilation (maximum).

Where the erosion for grey scale morphology can be defined as follow [11]:

$$[f \ominus b](x, y) = \min \{f(x + s, y + t)\}, \text{ where } (s, t) \in \mathcal{B} \quad (2)$$

And the dilation for grey scale morphology can be defined as follow [11]:

$$[f \oplus b](x, y) = \max \{f(x - s, y - t)\}, \text{ where } (s, t) \in \mathcal{B} \quad (3)$$

Where  $f \dots$  is the grey scale image.

$b \dots$  is the flat structuring element.

Moreover, the expressions for the opening and closing grey scale images can be defined as shown in Eq. (4) and Eq. (5) respectively [11].

$$f \circ b = (f \ominus b) \oplus b \quad (4)$$

$$f \bullet b = (f \oplus b) \ominus b \quad (5)$$

#### **3.2 Morphological despeckling filters**

The most common morphological filters that are used in speckle noise reduction are: morphological opening which can be easily expressed in terms of the value-and-criterion filter as both V and C is the minimum (erosion) operator and S is the maximum (dilation) operator respectively [6]. Morphological closing which can be easily expressed in terms of the value-and-criterion filter as both V and C is the maximum

(dilation) operator and S is the minimum (erosion) operator [6]. Finally, Tophat filter which is a close-open filter i.e. it consists of two stages where the first stage will be morphology closing. So it consists of two steps dilation followed by erosion with the same structuring element. The second stage will be morphology opening. So it consists of also two steps dilation to the output of first stage followed by erosion with the same structuring element of first stage. For speckle reduction, morphological tools perform even better than classical filters in preserving edges, saving the mean value of the image and computational time according to ease of implementation [12].

#### **4. The Proposed Morphological Filter**

In this technique we are still talking about the morphological filter which is based on a combination of two basic operators of mathematical morphology (erosion and dilation). Consequently, our proposed method consists of two stages like Tophat filter but it has two differences. (1) The operations that will be performed in the two stages will be chosen automatically according to the histogram of input SAR images. (2) The first stage consists of two operations (like Tophat filter) but the second stage consists of only one operation. This reduces the computational time and makes the implementation more easily. Thus, the sequence of the proposed filter operations are not rigid but it depends on the histogram of the noisy SAR image and its mean grey scale level, it consists of closing followed by erosion (i.e. dilation followed by two erosion operations) or opening followed by dilation (i.e. erosion followed by two dilation operations). The first sequence will be chosen if the histogram is concentrated in the first half. However the second sequence will be performed if the histogram is concentrated in the second half. Thus, we can say that this novel filter is adaptable according to the noisy SAR image contrast in selecting the sequence of operations. The order of the filter sequence gives the filter a great advantage in keeping a lot of details and preserving information.

#### **5. Experimental Results and Error Analysis**

Before beginning the analysis stage, we have to define our parameters that have been used in the evaluation of the filters. There are four parameters [13]:

**a- Target To Background Ratio (TTBR)** which equals

$$TTBR = (10 \log \frac{\sigma_T^2}{\sigma_B^2}) \tag{6}$$

Where  $\sigma_T^2$  ..... is the variance of the target.  $\sigma_B^2$  ..... is the variance of the background.

As this ratio increases as the detection and separation of targets become easier.

**b- Normalized mean (NM)**, to examine the ability to preserve the mean of a homogeneous regions which equals

$$NM = \frac{\mu_{\text{filter}}}{\mu_{\text{original}}} \quad (7)$$

Where  $\mu_{\text{filter}}$  and  $\mu_{\text{original}}$  are the means of the background segments of the filtered and the original image, respectively. The closer NM to 1, the better the filter ability to preserve the mean.

**c- Standard deviation to mean (STM)**, to determine the ability to reduce speckle noise of a homogeneous background segment which equals

$$STM = \frac{B}{\mu_{\text{filter}}} \quad (8)$$

Where  $B \dots$  is the standard deviation of filtered background and  $\mu_{\text{filter}} \dots$  is the mean of filtered background. So smaller STM, indicates a better speckle reduction ability.

**d- Edge Index (EI)**, to examine the ability to preserve detailed edge information which equals

$$EI = \frac{\sum P_f(i, j) - P_f(i-1, j+1)}{\sum P_o(i, j) - P_o(i-1, j+1)} \quad (9)$$

Where  $P_f(i, j)$  and  $P_o(i, j)$  are the filter and the original pixel values, respectively, of the edges of the selected background segment, with row number  $i$  and column number  $j$ . When  $EI=1$  the edge information is similar to the original image, edge blurring occurs for  $EI<1$ , and  $EI>1$  indicates edge enhancement.

Now we are going to test the mentioned filters plus the proposed morphological filter on two intensity noisy SAR images. Image (1) shows a desert region with some tanks as shown in figure 1 and its corresponding histogram is shown in figure 2. Moreover, Image (2) shows a grass region with some cars as shown in figure 3 and its corresponding histogram is shown in figure 4.

Samples of the output SAR images of the mentioned filters are shown in figures (5) and figures (6) to show the amount of enhancement achieved by each filter separately. From these samples we can see that the proposed filter has better achievement in preserving the details of targets and information in the images. Moreover, the output of the proposed filter maintains the details of the small regions that have been cancelled by other filters.

The resultant measurements parameters have been listed in table (1) to show the effect of different filters on noisy SAR images.

From table 1, we can see that all the mean, median and MCV filters introduce good values for speckle reduction and show good enhancement in TTBR parameter. However, they have blurred the edges according to EI parameter shown.

From table 1, we can see that both NM and EI values are in the defined ranges in the case of 3\*3 filter mask. we can consider that the Tophat (CO) filter has the best speckle reduction ability for morphological filters.

According to the fundamental nature of the SAR images, those are considered to be low contrast image. We found that if we remove the last step of the Tophat (CO) filter (i.e. dilation operation of the opening stage), we can get better results from this new filter (closing followed by erosion operation). From tables of the results, we can see that the novel filter has the smallest value for STM parameter, quiet high value for TTBR parameters like Mean filter and keeping NM and EI in their defined range. But for large filter mask the blurring in the edges will appear faster than the other filters (Mean and Median), this is due to the nature of high resolution SAR images which represent multiple object points in a single image pixel.

## **6. Conclusions**

Radar imageries are useful sources of information for roughness, geometry, and moisture content of the Earth surface. As an active, day/night, and all-weather remote sensing system, RADAR imageries can provide us with information for both surface and subsurface of the Earth. Speckle noise is added with RADAR imageries which gives a grainy appearance to the imageries. Speckle noise reduces the image contrast and has a negative effect on texture based analysis. Moreover, as speckle noise changes the spatial statistics of the images, it makes the classification process a difficult task to do. Thus, in order to get information out of RADAR imageries one should first remove/reduce the effect of speckle noise.

This paper reviewed the effect of applying a number of different filters plus new mathematical morphology on real SAR imageries. To measure the effect and the performance of the filters, four parameters are used. A good filter shows high TTBR, high NM Ratio, low STM value, and EI closer to one.

So we can conclude that the main advantages of the proposed morphological filter are: 1) Increasing target to background ratio more than the Tophat filter and closer to mean filter. 2) Achieving the smallest value for standard deviation to mean ratio (STM) i.e. is the best one in speckle reduction SAR images. 3) Keeping a good ratio for normalized

mean parameter i.e. the filtered image keeps almost information of the SAR .The main disadvantage of the new improved method is low value for edge index parameter (EI) for large filter window i.e. output image will be more blurred than the output images of the others filters because of high resolution of SAR images.

This work will be extended to use the proposed mathematical morphology filter to perform new adaptive filter in the near future.

### **References:**

- [1] C. Oliver and S. Quegan, *Understanding Synthetic Aperture Radar Images*, 1<sup>st</sup> ed., SciTech, INC., 2004.
- [2] D. Massonnet and J. Souyris, *Imaging with Synthetic Aperture Radar*, 1<sup>st</sup> ed., EPFL Press, 2008.
- [3] B. Tso and P. Mather, *Classification Methods for Remotely Sensed Data*, 2<sup>nd</sup> ed., CRC Press, 2000.
- [4] G. Franceschetti and R. Lanari, *Synthetic Aperture Radar Processing*, CRC Press, 1999.
- [5] R. Gonzalez and R. Woods, *Digital Image Processing*, 3<sup>rd</sup> ed., Addison-Wesley INC, 2008.
- [6] M. Schulze and J. Pearce, *Value-and-Criterion Filters: A new filter structure based upon Morphological opening and closing*, Nonlinear Image Processing IV, Proc. SPIE, Vol. 1902, P.106-115, 1993.
- [7] M. Schulze and Q. Wu, *Noise Reduction In Synthetic Aperture Radar Imagery Using A Morphology Based Nonlinear Filter*, Digital Image Computing: Techniques and Applications, P. 661-666, 1995.
- [8] G. Matheron, *Random Sets and Integral Geometry*, New York: Wiley, 1975.
- [9] J. Serra, *Image Analysis and Mathematical Morphology*, New York: Academic, 1982.
- [10] P. Maragos and R. Schafer, *Morphological Filters-Part I: Their Set-Theoretic Analysis and Relations to Linear Shift-Invariant*, IEEE Transaction on Acoustic, Speech, and Signal Processing, Vol. ASSP-35, No. 8, August 1987.
- [11] F. Shih, *Image Processing and Mathematical Morphology Fundamentals and Applications*, 1<sup>st</sup> ed., CRC Press, 2009.
- [12] A. Gasull and M. A. Herrero, *Oil Spills Detection In SAR Images Using Mathematical Morphology*, Proceedings of EUSIPCO, Toulouse, France, September 3-6, 2002.
- [13] Huang and S. Liu, *Some Uncertain Factor Analysis and Improvement In Spaceborne Synthetic Aperture Radar Imaging*. Signal Processing, Vol. 87, P. 3202-3217, 2007.





**Figure (1):** Original SAR image(1) (intensity noise image) of a desert region with some tanks

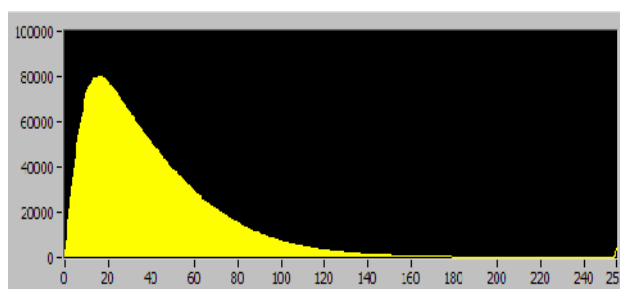


**Figure (2):** Histogram of SAR image(1)(intensity noise image)



**Figure (3):** Original SAR image(2) (intensity noise image) of a grass region with some cars

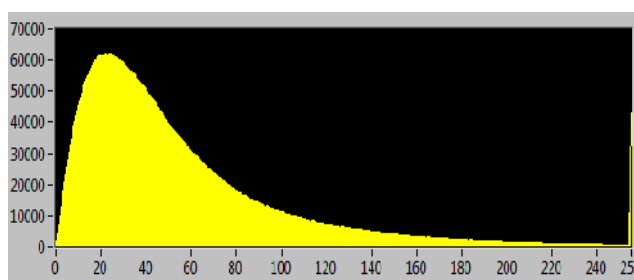


**Figure (4):** Histogram of SAR database (2) (intensity noise image)

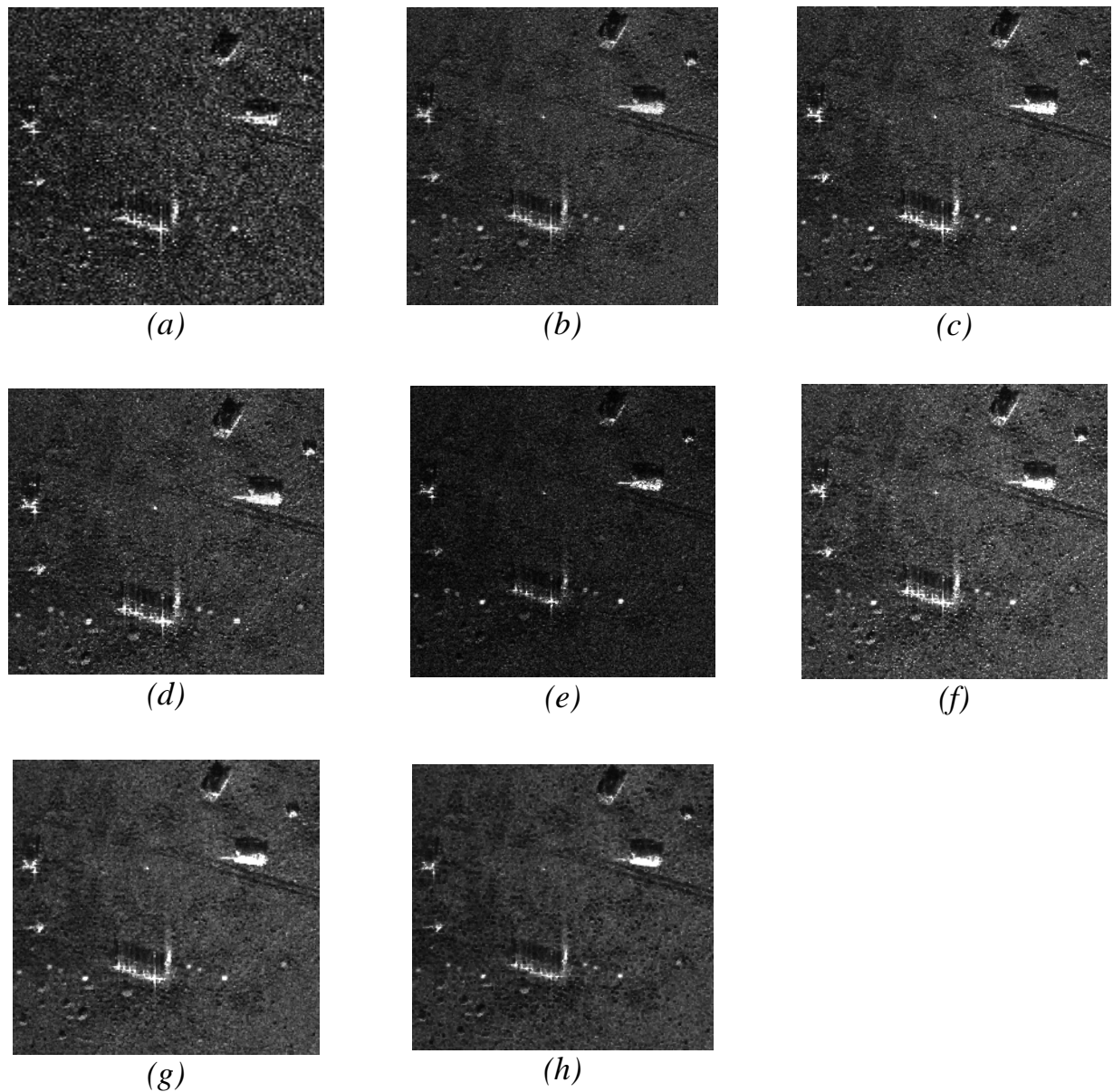


**Figure (5):** (a) Noisy SAR image (1), (b) (3\*3) Mean filtered image, (c) (3\*3) Median filtered image, (d) (3\*3) MCV filtered image, (e) (3\*3) Opening filtered image, (f) (3\*3) Closing filtered image, (g) (3\*3) Tophat filtered image, (h) (3\*3) Proposed Mathematical Morphology filtered image.

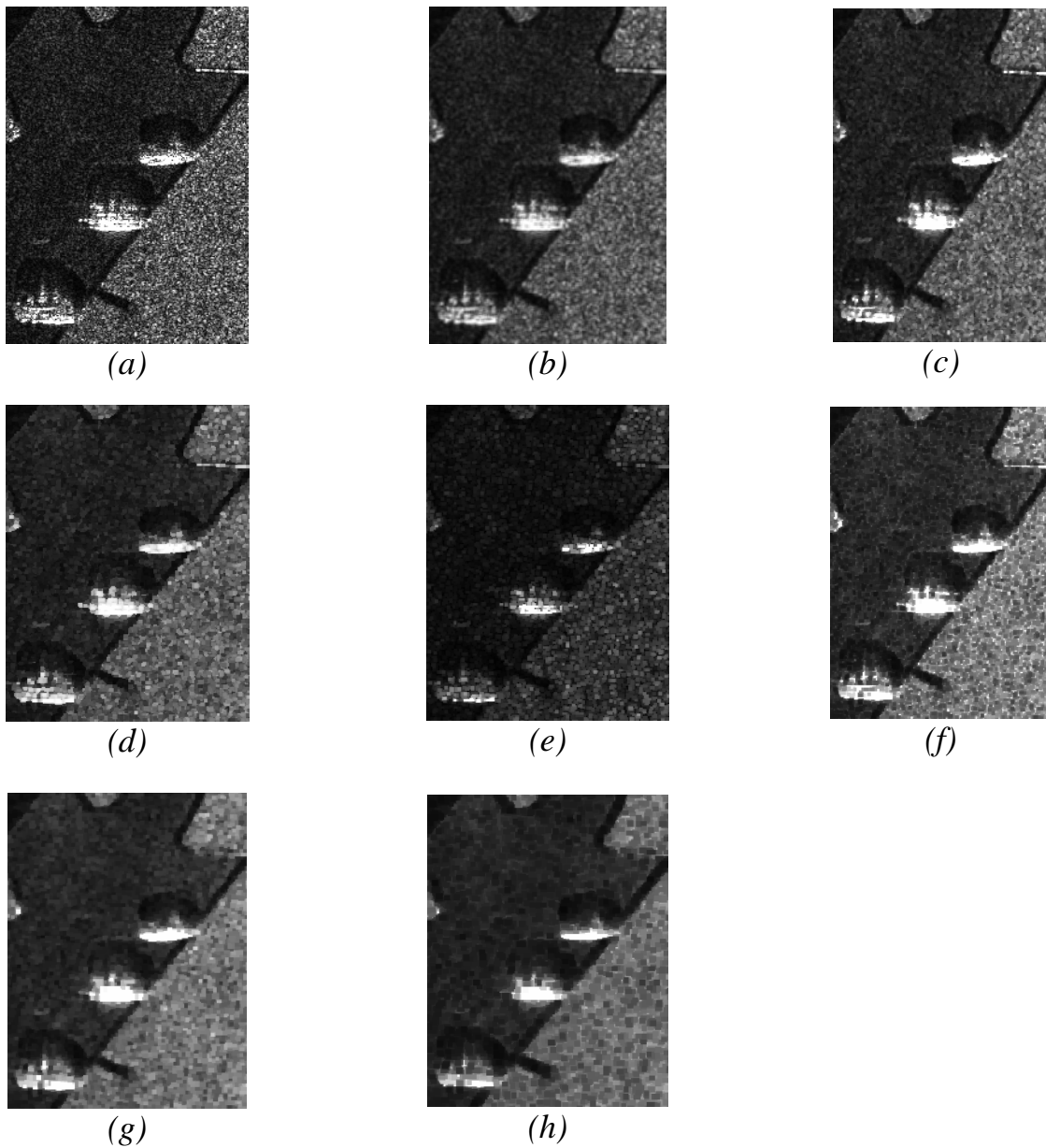


**Figure (6):** (a) Noisy SAR image (1), (b) (3\*3) Mean filtered image, (c) (3\*3) Median filtered image, (d) (3\*3) MCV filtered image, (e) (3\*3) Opening filtered image, (f) (3\*3) Closing filtered image, (g) (3\*3) Tophat filtered image, (h) (3\*3) Proposed Mathematical Morphology filtered image.

**Table (2): Comparison Measurements for different filtered images using filter mask (3\*3)**

FILTER	IMAGE (1) WITH TTBR = 9.33029				IMAGE (2) WITH TTBR = 4.59241			
	TTBR	NM	STM	EI	TTBR	NM	STM	EI
<b>MEDIAN FILTER</b>	13.1	1.10	0.31	0.88	8.928	1.10	0.26	0.87
<b>MEAN FILTER</b>	13.4	0.99	0.28	0.97	9.467	0.99	0.23	0.96
<b>MCV FILTER</b>	13.2	1.06	0.31	0.76	9.062	1.04	0.27	0.77
<b>CLOSING FILTER</b>	11.4	1.35	0.29	0.77	6.861	1.38	0.26	0.74
<b>OPENING FILTER</b>	15.6	0.57	0.43	0.73	11.35	0.55	0.40	0.72
<b>TOPHAT (CO) FILTER</b>	15.5	1.23	0.20	0.61	10.71	1.26	0.18	0.59
<b>PROPOSED FILTER</b>	16.2	1.09	0.21	0.59	11.49	1.13	0.19	0.57